*Inorg. Chem.* **2003**, *42*, 5523–5530

# Isolation and Structural Characterization of Anionic and Neutral Compounds Resulting from the Oxidative Addition of HI or $CH_3I$ to $[IrI_2(CO)_2]^-$

**Samuel Gautron,[†] Roberto Giordano,[†] Carole Le Berre,[†] Joël Jaud,[‡] Jean-Claude Daran,[§] Philippe Serp,[†] and Philippe Kalck*,[†]**

*Laboratoire de Catalyse, Chimie Fine et Polymères, Ecole Nationale Supérieure des Ingénieurs en Arts Chimiques et Technologiques, 118 route de Narbonne, 31077 Toulouse Cedex 4, France, Centre d'Elaboration des Matériaux et Etudes Structurales, BP 4347, 31055 Toulouse Cedex, France, and Laboratoire de Chimie de Coordination du CNRS, 205 route de Narbonne, 31077 Toulouse Cedex, France*

Received January 29, 2003

The active iridium species in the methanol carbonylation reaction has been crystallized as the $[PPN][IrI_2(CO)_2]$ complex and the X-ray structure solved, showing a cis-geometry and a square planar environment. Hydriodic acid reacts very quickly with this compound to provide $[PPN][IrHI_3(CO)_2]$, the X-ray crystal structure of which has been determined. The two CO ligands remain in mutual cis-position in a pseudooctahedral environment. The same cis-arrangement has been observed from the X-ray structure for $[PPN][IrI_3(CH_3)(CO)_2]$ resulting from the slower oxidative addition of $CH_3I$ to $[PPN][IrI_2(CO)_2]$. By iodide abstraction with $InI_3$, the anionic methyl complex gave rise to the dimeric neutral complex $[Ir_2(\mu\text{-}I)_2I_2(CH_3)_2(CO)_4]$. An X-ray structure showed that the methyl ligands are in the equatorial positions of the two octahedrons sharing an edge, formed by the two bridging iodide ligands. All these four complexes have been fully characterized by mass spectrometry, $^1H$ and $^{13}C$ NMR, and infrared both in solution and in the solid state. When necessary, the $^{13}CO$- or $^{13}CH_3$-enriched complexes have been prepared and analyzed.

## Introduction

The square-planar 16-electron $d^8$-complex *cis*-$[IrI_2(CO)_2]^-$ (anion of **1**) is an intermediate species in the iridium−ruthenium CATIVA process for methanol carbonylation,[1] in that it undergoes a rapid oxidative addition by methyl iodide to afford $[IrI_3(CH_3)(CO)_2]^-$, the resting state in the catalytic cycle. This iridium(I) complex was originally and independently proposed as the active catalytic species operating in the reaction mixtures by Forster[2] and Pannetier.[3]

The mechanistic feature that distinguishes the Ir-catalyzed reaction from the classical Rh-based Monsanto process, as far as the oxidative addition of MeI to the metallic center is concerned, is a much faster addition to Ir(I) than to Rh(I), while the rate of migration of the methyl group onto the coordinated CO ligand is $10^5-10^6$ higher for Rh(III) than for Ir(III).[4]

Forster[5] proposed that two catalytic cycles do coexist, one involving anionic and the other neutral iridium iodo carbonyl complexes, and that the predominance of one over the other could depend on iodide-ion levels and particularly HI concentration.[6] Variables such as water, methanol, and MeI content do furthermore influence which of the two cycles is likely to make the major contribution; the possibility of a competitive water-gas shift reaction should not be disregarded as well.

* To whom correspondence should be addressed. E-mail: Philippe.Kalck@ensiacet.fr. Tel: 0033562885690. Fax: 0033562885600.

[†] Ecole Nationale Supérieure des Ingénieurs en Arts Chimiques et Technologiques.

[‡] Centre d'Elaboration des Matériaux et Etudes Structurales.

[§] Laboratoire de Chimie de Coordination du CNRS.

(1) Haynes, A.; Mann, B. E.; Morris, G. E.; Maitlis, P. M. *J. Am. Chem. Soc*. **1993**, *115*, 4093.

(2) Forster, D. *J. Am. Chem. Soc*. **1976**, *98*, 846.

(3) Brodzki, D.; Denise, B.; Pannetier, G. *J. Mol. Catal*. **1977**, *2*, 149.

(4) (a) Bassetti, M.; Monti, D.; Haynes, A.; Pearson, J. M.; Stanbridge, I. A.; Maitlis, P. M. *Gazz. Chim. Ital.* **1992**, *122*, 391. (b) Griffin, T. R.; Cook, D. B.; Haynes, A.; Pearson, J. M.; Monti, D.; Morris, G. E. *J. Am. Chem. Soc*. **1996**, *118*, 3029. (c) Ellis, P. R.; Pearson, J. M.; Haynes, A.; Adams, H.; Bailey, N. A.; Maitlis, P. M. *Organometallics* **1994**, *13*, 3215. (d) Maitlis, P. M.; Haynes, A.; Sunley, G. J.; Howard, M. J. *J. Chem. Soc., Dalton Trans.* **1996**, 2187.

(5) Forster, D. *J. Chem. Soc., Dalton Trans*. **1979**, 1639.

(6) (a) Forster, D. *Adv. Organomet. Chem*. **1979**, *17*, 255. (b) Forster, D.; Hershman, A.; Morris, D. E. *Catal. Rev.—Sci. Eng*. **1981**, *23*, 89.

10.1021/ic0340938 CCC: $25.00 
Published on Web 08/08/2003

Three different regimes were envisaged, all of them pointing to the very important role played by iodide concentration in determining whether an anionic or a neutral catalytic cycle is actually operating.[7] In addition, the importance of $I^-$ concentration, first recognized to exert a powerful catalytic effect on the rate of the oxidative addition of alkyl halides to Rh(I) complexes,[8] was also observed in $H^+$ containing mixtures in which HI is generated. In fact, HI is able to compete with MeI, giving in its turn oxidative addition onto $[IrI_2(CO)_2]^-$ to form the hydride $[IrHI_3(CO)_2]^-$.[5] More recently, Ghaffar et al.[9] and Churlaud et al.[10] detected the latter hydridic species in their reaction mixtures under catalytic conditions, thus confirming the early proposal by Forster.[5] In their study, Churlaud et al.[10] reported that when the temperature is raised, $[IrHI_3(CO)_2]^-$ slowly gives $[IrI_4(CO)_2]^-$ and restores $[IrI_2(CO)_2]^-$ after $H_2$ evolution as previously pointed out.[5] Both *cis*-$[IrI_2(CO)_2]^-$ and the aforementioned hydrido iodo carbonyl species, together with $[IrI_3(CO)_3]$,[11] are involved in the water-gas shift reaction, which represents a significant side reaction in the methanol carbonylation process.[11,12a,b]

As far as halo carbonyl complexes of iridium are concerned, oxidative addition reactions onto $[IrX_2(CO)_2]^-$ anions were studied with regard to either mechanism and stereochemical course.[12,13] Interestingly, hydrogen halides were found to add to the square-planar Ir(I) complexes in a stereospecific cis-fashion: the geometry of the oxidative addition-derived iridium complexes is *fac*,*cis* while the same reactions onto $[RhI_2(CO)_2]^-$ afford *mer*,*trans* analogues.

The major formal difference between the oxidative addition of HI and that of MeI consists of a mechanistic one. Indeed, the first step of the former process is the protonation of the electron-rich iridium center via an electrophilic addition, which explains the faster reaction rate observed for HI; by contrast, kinetic evidence and theoretical calculations[4a,b] indicate a classical $S_N2$ reaction pathway for MeI, by which the nucleophile *cis*-$[IrI_2(CO)_2]^-$ slowly attacks the carbon atom, giving rise to a linear transition state with iodide as a leaving group. Moreover, a density functional study of the oxidative addition of MeI onto the Ir(I) precursor[14a,b] showed that the only cis form of $[IrI_2(CO)_2]^-$ undergoes this type of reaction.[4c] On energy grounds the trans isomer would react faster than the cis one (the difference in energy being 3.7 kcal in favor of the trans form), but that is not the case since the cis to trans conversion is unlikely to occur (difference in energy of 10.39 kcal, the cis isomer being the more stable).

Therefore, we were interested in studying the competition between HI and MeI for *cis*-$[IrI_2(CO)_2]^-$ and to determine the structures of the so-generated anionic complexes.

Furthermore, anionic dimeric halogeno carbonyls of iridium have been known for many years,[15] and neutral dimeric complexes such as $[Ir(\mu\text{-}Cl)Cl(CH_3)(CO)_2]_2$[16] and $[Ir(\mu\text{-}Cl)(Cl)H(CO)_2]_2$[17] were also prepared. As the neutral dimeric complex $[Ir(\mu\text{-}I)I(CH_3)(CO)_2]_2$ has been reported[18] to react with CO to give the tricarbonyl species $[IrI_2(CH_3)(CO)_3]$, an intermediate in the iridium-catalyzed methanol carbonylation, our goal was also to synthesize the related iridium dinuclear complexes that could be generated from the Ir(III) anionic species detected and/or isolated in the course of this work, via reaction with iodide-abstraction agents.

## Experimental Section

**General Procedures.** All manipulations were carried out with standard vacuum and dry-argon techniques. Dimethylformamide (DMF, Scharlau, 99.8%), iodomethane ($CH_3I$, Acros, 99%), hydriodic acid (HI, Merck, 57%), indium triodide ($InI_3$, Acros, 99.9%), *n*-hexane (Scharlau, 96%), $IrI_3$ (iridium iodide (Johnson-Mathey) is sold as $IrI_{3.4}$, which is a mixture of $IrI_3$ and $IrI_4$), and carbon C-13-enriched carbon monoxide (Air Liquide, 99%) were used as received, and dichloromethane ($CH_2Cl_2$, Aldrich) was dried with $CaH_2$. $^1H$ and $^{13}C$ spectra were recorded with Bruker AC250 or AMX 400 spectrometers. Mass spectra were recorded on a NERMAG R10-10 (FAB negative mode; gas: Xe). The reference for the NMR chemical shifts was $SiMe_4$. Solution infrared spectra were recorded on a Perkin-Elmer 1710 spectrophotometer with a 0.1 mm cell equipped with $CaF_2$ windows and when necessary with a high-pressure infrared cell (Autoclave Top Industrie).

**X-ray Crystallographic Study.** Data for compounds **1**, **3**, and **4** were collected on an Oxford-Diffraction Xcalibur diffractometer whereas a Nonius Kappa CCD was used for compound **2**. The final unit cell parameters were obtained by the least-squares refinement of a large number of selected reflections. For all compounds, only statistical fluctuations were observed in the intensity monitors over the course of the data collections.

The structure was solved by direct methods (SIR97)[19] and refined by least-squares procedures on $F^2$. In all compounds, all H atoms were introduced at calculated positions as riding atoms [$d$(CH) = 0.99−0.98 Å], using AFIX43 for $C_6H_5$ and AFIX137 for $CH_3$ groups, with a displacement parameter equal to 1.2 ($C_6H_5$) or 1.5 ($CH_3$) times that of the parent atom. In compound **3**, one of the CO's and the methyl were disordered on two sites with an occupation factor ratio of 0.67/0.33. Least-squares refinements were carried out by minimizing the function $\Sigma w(F_o^2 - F_c^2)^2$, where $F_o$ and $F_c$ are the observed and calculated structure factors. The weighting scheme used in the last refinement cycles was $w = 1/[\sigma^2(F_o^2) + (aP)^2 + bP]$, where $P = (F_o^2 + 2F_c^2)/3$. Models reached convergence with $R = \Sigma(||F_o| - |F_c||)/\Sigma(|F_o|)$ and wR2 $= \{\Sigma w(F_o^2 - F_c^2)^2/\Sigma w(F_o^2)^2\}^{1/2}$, having values listed in Table 1.


(7) Forster, D.; Singleton, T. C. *J. Mol. Catal*. **1982**, *17*, 299.
(8) Forster, D. *J. Am. Chem. Soc*. **1975**, *97*, 951.
(9) Ghaffar, T.; Charmant, J. P. H.; Sunley, G. J.; Morris, G. E.; Haynes, A.; Maitlis, P. M. *Inorg. Chem. Commun*. **2000**, *3*, 11.
(10) Churlaud, R.; Frey, U.; Metz, F.; Merbach, A. E. *Inorg. Chem*. **2000**, *39*, 4137.
(11) Jones, J. H. *Platinum Met. Rev*. **2000**, *44*, 94.
(12) (a) Forster, D. *Inorg. Chem*. **1972**, *11*, 473. (b) Haak, S.; Haynes, A.; Maitlis, P. M.; Morris, G. E.; Watt, R. J. *12th International Symposium on Homogeneous Catalysis*, Stockholm, Sweden, Aug 23−29, 2000.
(13) Haynes, A.; McNish, J.; Pearson, J. M. *J. Org. Chem.* **1998**, *551*, 339.
(14) (a) Kinnunen, T.; Laasonen, K. *J. Mol. Struct. (THEOCHEM)* **2001**, *542*, 273. (b) Kinnunen, T.; Laasonen, K. *J. Mol. Struct. (THEOCHEM)* **2001**, *540*, 91.
(15) Cleare, M. J.; Griffith, W. P. *J. Chem. Soc. A* **1970**, 2788.
(16) Bailey, N. A.; Jones, C. J.; Shaw, B. L.; Singleton, E. *Chem. Commun*. **1967**, 1051.
(17) Shaw, B. L.; Singleton, E. *J. Chem. Soc. A* **1967**, 1683
(18) Ghaffar, T.; Adams, H.; Maitlis, P. M.; Sunley, G. J.; Baker, M. J.; Haynes, A. *Chem. Commun.* **1998**, 1023.
(19) Altomare, A.; Burla, M. C.; Camalli, M.; Cascarano, G. L.; Giacovazzo, C.; Guagliardi, A.; Moliterni, A. G. G.; Polidori, G.; Spagna, R. SIR97 a program for automatic solution of crystal structures by direct methods. *J. Appl. Crystallogr*. **1999**, *32*, 115.

**Table 1.** Crystal Data and Structure Refinement Parameters

| param | **1** | **2** |
|---|---|---|
| empirical formula | $C_{38}H_{30}I_2IrNO_2P_2$ | $C_{38}H_{31}I_3IrNO_2P_2$ |
| fw | 1040.57 | 1168.48 |
| temp, K | 180(2) | 293(2) |
| wavelength, Å | 0.710 73 | 0.710 73 |
| cryst system | triclinic | monoclinic |
| space group | $P\bar{1}$ | $P2_1/c$ |
| *a*, Å | 10.0352(15) | 9.3661(3) |
| *b*, Å | 17.363(2) | 16.4735(6) |
| *c*, Å | 21.899(3) | 25.2247(5) |
| α, deg | 76.120(10) | 90.0 |
| *β*, deg | 88.430(10) | 94.713(2) |
| *γ*, deg | 80.460(10) | 90.0 |
| *V*, Å$^3$ | 3652.7(8) | 3878.8(2) |
| *Z* | 4 | 4 |
| *D*(calcd), Mg/m$^3$ | 1.892 | 2.001 |
| abs coeff, mm$^{-1}$ | 5.467 | 5.945 |
| *F*(000) | 1976 | 2192 |
| cryst size, mm | 0.34 × 0.07 × 0.063 | 0.15 × 0.17 × 0.20 |
| *θ* range, deg | 3.41−25.68 | 2.58−27.46 |
| index ranges | $-7 \le h \le 12$, $-21 \le k \le 21$, $-26 \le l \le 26$ | $0 \le h \le 12$, $0 \le k \le 21$, $-32 \le l \le 32$ |
| reflecns collcd | 26 163 | 9607 |
| unique reflecns ($R_{int}$) | 13 731 (0.0796) | 8852 (0.063) |
| completeness, % | 98.9 | 99.6 |
| abs corr | analytical | semiempirical |
| max and min transm | 0.578 and 0.876 | 0.541 and 0.378 |
| data/restraints/params | 13 731/730/829 | 8852/0/428 |
| goodness-of-fit on $F^2$ | 0.911 | 0.801 |
| final R indices [$I > 2\sigma(I)$] | R1 = 0.0580, wR2 = 0.0930 | R1 = 0.0399, wR2 = 0.0799 |
| R indices (all data) | R1 = 0.1245, wR2 = 0.1137 | R1 = 0.0820, wR2 = 0.0942 |
| resid density, e Å$^{-3}$ | 1.236 and −1.973 | 1.014 and −1.281 |

| param | **3** | **4** |
|---|---|---|
| empirical formula | $C_{39}H_{33}I_3IrNO_2P_2 \cdot CH_2Cl_2$ | $C_3H_3I_2IrO_2$ |
| fw | 1267.43 | 517.05 |
| temp, K | 180(2) | 180(2) |
| wavelength, Å | 0.710 73 | 0.710 73 |
| cryst system | monoclinic | triclinic |
| space group | $P2_1/c$ | $P\bar{1}$ |
| *a*, Å | 10.6554(5) | 6.6629(18) |
| *b*, Å | 26.6621(14) | 7.6766(19) |
| *c*, Å | 14.9769(9) | 8.710(2) |
| α, deg | 90.0 | 102.94(2) |
| *β*, deg | 98.809(4) | 110.72(3) |
| *γ*, deg | 90.0 | 90.52(2) |
| *V*, Å$^3$ | 4204.7(4) | 404.19(18) |
| *Z* | 4 | 2 |
| *D*(calcd), Mg/m$^3$ | 2.002 | 4.248 |
| abs coeff, mm$^{-1}$ | 5.616 | 24.078 |
| *F*(000) | 2392 | 440 |
| cryst size, mm | 0.317 × 0.317 × 0.186 | 0.204 × 0.138 × 0.057 |
| *θ* range, deg | 2.99−26.31 | 4.07−26.37 |
| index ranges | $-9 \le h \le 13$, $-33 \le k \le 33$, $-18 \le l \le 18$ | $-8 \le h \le 8$, $-9 \le k \le 9$, $-10 \le l \le 10$ |
| reflecns collcd | 29 700 | 2468 |
| unique reflecns ($R_{int}$) | 8588 (0.0360) | 1541 (0.0461) |
| completeness, % | 99.8 | 93.1 |
| abs corr | analytical | analytical |
| max and min transm | 0.6059 and 0.3207 | 0.2578 and 0.0726 |
| data/restraints/params | 8588/421/491 | 1541/0/75 |
| goodness-of-fit on $F^2$ | 0.956 | 1.084 |
| final R indices [$I > 2\sigma(I)$] | R1 = 0.0322, wR2 = 0.0641 | R1 = 0.0338, wR2 = 0.0874 |
| R indices (all data) | R1 = 0.0471, wR2 = 0.0683 | R1 = 0.0385, wR2 = 0.0900 |
| resid density, e Å$^{-3}$ | 1.170 and 1.095 | 1.437 and 1.875 |

The calculations were carried out with the SHELXL-97 program[20] using the integrated system WINGX(1.63).[21] A molecular view was realized with the ORTEP program.[22] Fractional atomic coordinates, anisotropic thermal parameters for non-hydrogen atoms, and atomic coordinates for H atoms have been deposited as Supporting Information.

**Synthesis of [PPN][$IrI_2(CO)_2$] (1).** In a two-necked flask (250 mL) equipped with gas inlet and a reflux condenser was placed 2 g (3.21 mmol) of $IrI_{3.4}$ in a mixture of DMF (150 mL) and water (1.5 mL); CO was passed through the stirred solution, and the temperature was raised to 160 °C. After 4 h, the solution color changed from dark to yellow. After the solution was cooled to room temperature, PPNCl was added (1 molar equiv/Ir) to the limpid solution; further addition of cold deionized water caused the precipitation of [PPN][$IrI_2(CO)_2$] (**1**). Careful washing of the resulting salt with water gave a yellow solid, which was dried in vacuo. Recrystallization from bilayered $CH_2Cl_2$/*n*-heptane gave yellow needles suitable for X-ray determination ($m$ = 1.67 g; yield: 50%). IR ($CH_2Cl_2$): 2046 (s), 1967 (s) cm$^{-1}$. IR (KI pellets): 2045 (s), 2034 (s), 1968 (s), 1960 (s) cm$^{-1}$. MS: $m/z$ = 503. $^{13}$C NMR ($CD_2Cl_2$): $\delta$ ppm 169.9 ppm (s, CO).

**Synthesis of [PPN][$IrHI_3(CO)_2$] (2).** Differently from the early report by Forster,[5] who prepared the above hydridoiridium species via the addition of slightly more than 1 equiv of HI to $[IrI_2(CO)_2]^-$ in nitromethane, we found that large amounts of $[IrI_4(CO)_2]^-$ were formed as a side product when adapting his synthetic procedure to $CH_2Cl_2$ reaction mixtures.

Hence we modified the synthetic method as follows: In a Schlenk tube, 20 mL of $CH_2Cl_2$ was placed and degassed with a flow of $N_2$ ; the [PPN][$IrI_2(CO)_2$] salt was added (500 mg; 0.48 mmol), and then HI was added dropwise with a microsyringe and very slowly to the well-stirred solution of the Ir(I) anion, while monitoring the disappearance of the reactant IR bands after every addition of HI. When the IR spectrum signaled that the reaction had reached completion, addition of HI was stopped and a bright orange-red limpid solution was obtained. The solution was evaporated and the residual dried in vacuo to afford an orange-red solid ($m$ = 549 mg; yield 98%), which was dissolved in 20 mL of degassed acetone; *n*-heptane was then slowly added to give a bilayered mixture suitable for recrystallization. Indeed, after 1 month at −18 °C, large dark orange crystals could be found, suitable for X-ray diffractometry; they were dried by bubbling $N_2$ through the solution and kept under inert atmosphere. IR ($CH_2Cl_2$): 2157 (vw, $\nu_{Ir-H}$), 2103, 2052 (s, $\nu_{CO}$) cm$^{-1}$. MS: $m/z$ = 631. $^1$H NMR ($CD_2Cl_2$): $\delta$ −11.65 ppm. $^{13}$C NMR ($CD_2Cl_2$): $\delta$ 155.0 ppm (s, CO).

**Synthesis of [PPN][$IrI_3(CH_3)(CO)_2$] (3).** In a 20 mL Schlenk tube 10 mL of $CH_2Cl_2$ was degassed with a flow of $N_2$; [PPN]-[$IrI_2(CO)_2$] (**1**) (1 g; 0.96 mmol) was added together with 40 equiv of $CH_3I$. After the mixture was stirred for 1 h at room temperature, an orange solution was obtained. Drying in vacuo afforded an orange solid. Recrystallization from a bilayered $CH_2Cl_2$/*n*-heptane mixture gave orange crystals suitable for X-ray analysis ($m$ = 0.68 g; yield 60%). IR ($CH_2Cl_2$): 2100 (s), 2048 (s) cm$^{-1}$. IR (KI pellets): 2088 (s), 2034 (s) cm$^{-1}$. MS: $m/z$ = 646. $^1$H NMR ($CD_2Cl_2$): $\delta$ 2.15 ppm. $^{13}$C NMR ($CD_2Cl_2$): $\delta$ 156.0 (s, CO), −15.75 ppm (s, $CH_3$).

(20) Sheldrick, G. M. *SHELX97, Programs for Crystal Structure Analysis (Release 97-2)*; Institüt für Anorganische Chemie der Universität: Tammanstrasse 4, D-3400 Göttingen, Germany, 1998.
(21) Farrugia, L. J. *J. Appl. Crystallogr.* **1999**, *32*, 837−838.
(22) (a) Burnett, M. N.; Johnson, C. K. *ORTEP-III;* Report ORNL-6895; Oak Ridge National Laboratory: Oak Ridge, TN, 1996. (b) Farrugia, L. J. ORTEP3 for Windows. *J. Appl. Crystallogr.* **1997**, *30*, 565.

**Synthesis of $[Ir_2(\mu\text{-}I)_2I_2(CH_3)_2(CO)_4]$ (4).** Addition of an equimolecular amount of $InI_3$ to a $CH_2Cl_2$ solution (20 mL) of $[PPN][IrI_3CH_3(CO)_2]$ (**3**) ($m = 2$ g; 1.69 mmol) and drying in vacuo, followed by extraction with hot cyclohexane from the $[PPN][InI_4]$ residual, afforded a dark orange solution. Drying in vacuo gave an orange solid that was dissolved in $CH_2Cl_2$ ; further addition of *n*-heptane afforded a bilayered mixture from which crystals were obtained after 1 week in the refrigerator (−20 °C) (0.22 g; yield 25%). IR ($CH_2Cl_2$): 2120 (s), 2074 (s) $cm^{-1}$. $^1H$ NMR ($CD_2Cl_2$): $\delta$ 1.96, 1.90 ppm. $^{13}C$ NMR ($CD_2Cl_2$): $\delta$ 152.5, 150.4, 150.1 ppm (CO).

## Results and Discussion

Since the iridium-based catalytic system for the carbonylation of methanol involves the production of MeI in aqueous acidic media through the reaction of HI on $CH_3OH$, we studied the reactivity of HI and of MeI toward the precursor *cis*-$[IrI_2(CO)_2]^-$. We at first followed the formation of the *cis*-$H[IrI_2(CO)_2]$ precursor by CO reduction of the iridium iodide salt in water-containing reaction mixtures. To compare their reactivity, we performed the oxidative addition reactions of HI and of MeI in chlorobenzene, which lead to the formation of the corresponding species $H[IrHI_3(CO)_2]$ and $H[IrI_3(CH_3)(CO)_2]$, respectively.

We could prepare, isolate, and crystallize these anionic complexes as their $PPN^+$ salts and determined their X-ray structures, together with that of the precursor $[PPN][IrI_2(CO)_2]$.

Starting from the above oxidative addition-derived anionic species, we also prepared, by reaction with $InI_3$, a iodide-abstraction agent, the neutral dimer $[Ir_2(\mu\text{-}I)_2(I)_2(CH_3)_2(CO)_4]$, fully characterized both by spectroscopy and X-ray diffractometry.

**$[PPN][IrI_2(CO)_2]$ (1).** The anionic iridium(I) precursor $[IrI_2(CO)_2]^-$, which directly intervenes in the catalytic cycle, curiously has never been described in the solid state. We succeeded in isolating and crystallizing this anionic complex as its $PPN^+$ salt.

Carbonylation of DMF solutions of $IrI_{3.4}$ affords quantitatively $[NH_2Me_2][IrI_2(CO)_2]$ after 3−4 h, as shown by infrared spectroscopy. The ammonium cation results from the decarbonylation of DMF and its protonation by HI.[23] After $PPN^+$ addition (see Scheme 1) and recrystallization from a $CH_2Cl_2$/*n*-heptane mixture, yellow needles of $[PPN][IrI_2(CO)_2]$ were obtained, suitable for X-ray crystal structure determination.

**Scheme 1.** Rapid Preparation of $[PPN][IrI_2(CO)_2]$ from a Commercial Iridium Salt

$$IrI_{3\cdot4} \xrightarrow[\text{DMF, } H_2O\text{, reflux, 3h}]{\text{CO (1 bar), 160°C}} [NH_2Me_2][IrI_2(CO)_2] \xrightarrow[2)\ H_2O,\ -[NH_2Me_2]Cl]{1)\ [PPN]Cl} [PPN][IrI_2(CO)_2]$$

**1**

Crystal data for complex $[PPN][IrI_2(CO)_2]$ (**1**) are listed in Table 1. Its X-ray structure is shown in Figure 1, and bond lengths and angles of interest are listed in Table 2.

The geometry of the above anionic species **1** presents a square-planar environment for the iridium metal center, and the two CO ligands are in a cis arrangement. Two nearly identical molecules coexist in the asymmetric unit; indeed,

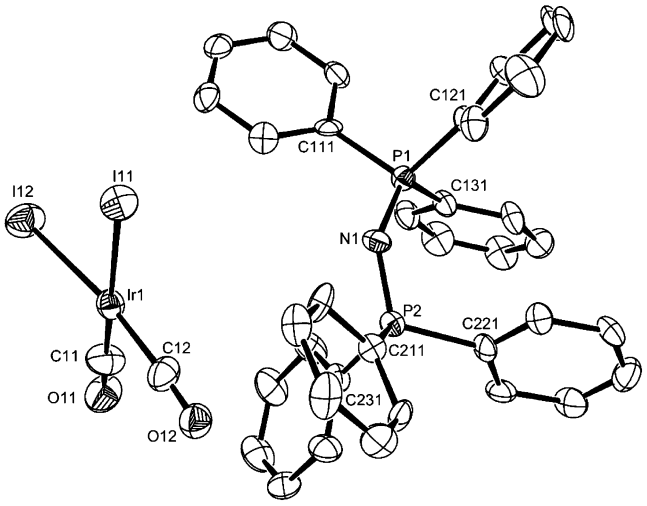


**Figure 1.** ORTEP view of $[PPN][IrI_2(CO)_2]$ (**1**) with atomic labeling scheme for the anion and showing mainly the two phosphorus and the nitrogen atoms of the cation. Ellipsoids are at the 50% probability level.

in molecule A the two Ir(1)−I(11) and Ir(1)−I(12) bond lengths correspond to 2.6755(10) and 2.6273(10) Å, respectively, which well accords with the Ir(2)−I(21) and Ir(2)−I(22) bond distances of 2.6581(11) and 2.6551(10) Å. In molecule B, the thermal parameters of one iodine atom appear to be larger than the other, whereas the CO ligand trans to this iodide presents ellipsoids smaller than expected. This phenomenon might be due to a disorder between $I^-$ and CO ligands. However, no correct model can be defined for this disorder. Apparently the isomer shown is present in greater than 90%. The four angles around the iridium atoms vary from 84.1(4) to 94.0(5)° and do therefore deserve some further discussion. The I−Ir−I values of 90.99(3) and 92.31(3)° are close to a right angle. The C(11)−Ir(1)−C(12) angle measures 94.0(5)°, the C(21)−Ir(2)−C(22) one reaches 91.9(6)°, and the values of 84.1(4)° for I(12)−Ir(1)−C(12) and 86.1(4)° for I(22)−Ir(2)−C(21) are essentially due to the lack of linearity along the Ir−C−O bonds.

The structure of the rhodium analogue complex $[PyMe][RhI_2(CO)_2]$ has been reported very recently.[24] In the two disordered structures solved with two different countercations, the bond distances and angles compare well with those found here, since the mean Rh−I distance is ca. 2.66 Å, Rh−C is 1.85 Å, and C−O is 1.125 Å.

The mean value calculated for the iridium−iodine bond length is 2.654 Å. It is worth mentioning that previous ab initio calculations carried out by Kinnunen and Laasonen[14] on *cis*-$[IrI_2(CO)_2]^-$ indicate a 2.778 Å value for both the Ir−I bond distances, i.e. 0.124 Å overestimated compared to that measured in this work.

IR spectra of KI pellets of $[PPN][IrI_2(CO)_2]$ show a pattern of four CO bands possessing almost the same intensity, at 2045, 2034, 1968, and 1960 $cm^{-1}$: they do actually correspond to two systems of two bands each, arising from the

(23) Serp, P.; Hernandez, M.; Richard, B.; Kalck, P. *Eur J. Inorg. Chem.* **2001**, 2327.
(24) Haynes, A.; Maitlis, P. M.; Quyoum, R.; Pulling, C.; Adams, H.; Spey, S. E.; Stange, R. W. *J. Chem. Soc., Dalton Trans.* **2002**, 2565.

**Table 2.** Bond Lengths (Å) and Bond Angles (deg) within the Anions with Esd's Referring to the Last Significant Digit

| Molecule A | | Molecule B | |
|---|---|---|---|
| | Compound **1** | | |
| Ir(1)−C(11) | 1.813(7) | Ir(2)−C(21) | 1.802(7) |
| Ir(1)−C(12) | 1.815(7) | Ir(2)−C(22) | 1.808(7) |
| Ir(1)−I(12) | 2.6268(10) | Ir(2)−I(22) | 2.6551(10) |
| Ir(1)−I(11) | 2.6759(10) | Ir(2)−I(21) | 2.6575(11) |
| O(11)−C(11) | 1.114(7) | O(21)−C(21) | 1.092(7) |
| O(12)−C(12) | 1.118(7) | O(22)−C(22) | 1.114(7) |
| C(11)−Ir(1)−C(12) | 92.2(5) | C(21)−Ir(2)−C(22) | 90.9(6) |
| C(11)−Ir(1)−I(12) | 84.6(4) | C(21)−Ir(2)−I(22) | 88.4(4) |
| C(12)−Ir(1)−I(12) | 173.3(4) | C(22)−Ir(2)−I(22) | 179.2(4) |
| C(11)−Ir(1)−I(11) | 174.2(4) | C(21)−Ir(2)−I(21) | 178.1(4) |
| C(12)−Ir(1)−I(11) | 92.6(4) | C(22)−Ir(2)−I(21) | 88.4(4) |
| I(12)−Ir(1)−I(11) | 91.00(3) | I(22)−Ir(2)−I(21) | 92.36(3) |
| O(11)−C(11)−Ir(1) | 177.3(12) | O(21)−C(21)−Ir(2) | 175.9(12) |
| O(12)−C(12)−Ir(1) | 176.2(11) | O(22)−C(22)−Ir(2) | 178.0(14) |
| | Compound **2** | | |
| Ir(1)−C(11) | 1.913(10) | Ir(1)−I(1) | 2.6964(6) |
| Ir(1)−C(12) | 1.858(8) | Ir(1)−I(2) | 2.6927(5) |
| C(11)−O(11) | 1.042(9) | Ir(1)−I(3) | 2.8360(6) |
| C(12)−O(12) | 1.127(8) | | |
| C(11)−Ir(1)−C(12) | 95.3(3) | C(12)−Ir(1)−I(2) | 171.4(2) |
| C(11)−Ir(1)−I(2) | 87.2(2) | C(12)−Ir(1)−I(1) | 84.7(3) |
| C(11)−Ir(1)−I(1) | 175.3(3) | C(11)−Ir(1)−I(3) | 88.9(3) |
| I(2)−Ir(1)−I(1) | 92.049(19) | C(12)−Ir(1)−I(3) | 96.7(2) |
| I(2)−Ir(1)−I(3) | 91.563(18) | I(1)−Ir(1)−I(3) | 95.749(18) |
| | Compound **3**[a] | | |
| I(1)−Ir(1) | 2.7005(4) | Ir(1)−C(11) | 1.870(5) |
| I(2)−Ir(1) | 2.7658(4) | C(11)−O(11) | 1.118(6) |
| I(3)−Ir(1) | 2.7177(4) | | |
| Ir(1)−C(12) | 1.830(10) | Ir(1)−C(12A) | 1.829(15) |
| Ir(1)−C(1) | 2.131(10) | Ir(1)−C(1A) | 2.156(16) |
| C(12)−O(12) | 1.132(11) | C(12A)−O(12 A) | 1.135(16) |
| O(11)−C(11)−Ir(1) | 178.0(5) | C(11)−Ir(1)−I(2) | 89.98(15) |
| C(12)−Ir(1)−C(11) | 92.6(6) | C(12A)−Ir(1)−C(11) | 94.9(9) |
| C(12)−Ir(1)−C(1) | 94.2(6) | C(12A)−Ir(1)−C(1A) | 91.7(9) |
| C(11)−Ir(1)−C(1) | 89.8(4) | C(11)−Ir(1)−C(1A) | 91.8(12) |
| C(12)−Ir(1)−I(1) | 87.7(6) | C(12A)−Ir(1)−I(1) | 82.0(9) |
| C(11)−Ir(1)−I(1) | 176.85(16) | C(11)−Ir(1)−I(3) | 87.82(16) |
| C(1)−Ir(1)−I(1) | 87.1(4) | C(1A)−Ir(1)−I(1) | 88.5(12) |
| C(12)−Ir(1)−I(3) | 179.5(6) | C(12A)−Ir(1)−I(3) | 87.6(8) |
| C(1)−Ir(1)−I(3) | 86.2(4) | C(1A)−Ir(1)−I(3) | 179.1(11) |
| I(1)−Ir(1)−I(3) | 91.885(12) | I(1)−Ir(1)−I(2) | 93.168(13) |
| C(12)−Ir(1)−I(2) | 86.2(6) | C(12A)−Ir(1)−I(2) | 175.0(9) |
| C(1)−Ir(1)−I(2) | 179.5(4) | C(1A)−Ir(1)−I(2) | 87.4(10) |
| O(12)−C(12)−Ir(1) | 176.7(16) | O(12A)−C(12A)−Ir(1) | 179(2) |
| I(3)−Ir(1)−I(2) | 93.397(14) | | |
| | Compound **4**[b] | | |
| Ir(1)−C(1) | 1.872(12) | Ir(1)−I(3) | 2.8021(11) |
| Ir(1)−C(2) | 1.872(12) | I(3)−Ir(1) | 2.8021(11) |
| Ir(1)−C(3) | 2.165(11) | O(2)−C(2) | 1.107(14) |
| Ir(1)−I(2) | 2.6874(11) | C(1)−O(1) | 1.123(15) |
| Ir(1)−I(3) | 2.7156(11) | | |
| C(1)−Ir(1)−C(2) | 96.3(5) | I(2)−Ir(1)−I(3)′ | 91.50(4) |
| C(1)−Ir(1)−C(3) | 87.7(5) | C(1)−Ir(1)−I(3) | 98.8(3) |
| C(2)−Ir(1)−C(3) | 89.6(4) | C(2)−Ir(1)−I(3) | 91.1(3) |
| C(1)−Ir(1)−I(2) | 85.6(4) | C(3)−Ir(1)−I(3) | 173.3(3) |
| C(2)−Ir(1)−I(2) | 177.4(4) | I(2)−Ir(1)−I(3) | 90.38(4) |
| C(3)−Ir(1)−I(2) | 88.7(3) | I(3)−Ir(1)−I(3)′ | 85.70(3) |
| C(1)−Ir(1)−I(3)′ | 174.7(4) | Ir(1)−I(3)−Ir(1)′ | 94.30(3) |
| C(2)−Ir(1)−I(3)′ | 86.4(4) | O(1)−C(1)−Ir(1) | 176.7(10) |
| C(3)−Ir(1)−I(3)′ | 87.7(3) | O(2)−C(2)−Ir(1) | 176.4(11) |

[a] A refers to the disordered distribution of $CH_3$ and CO. [b] Symmetry transformations used to generate equivalent atoms: ′, $-x+1$, $-y+1$, $-z+1$.

two slightly different iridium moieties observed in the unit cell in their environment, both of them having a cis-arrangement of the ligands, and definitely not from the presence of the trans isomer, never detected in the course of this study. Indeed, dissolution of the solid material in dichloromethane, monitored by infrared spectroscopy, does only afford the two CO bands at 2046(s) and 1967(s) $cm^{-1}$, peculiar to the cis-complex in solution. In $^{13}C$ NMR spectra the two equivalent CO ligands appear as one singlet at 169.9 ppm, in $CD_2Cl_2$ solution.

Moreover, in the absence of a stabilizing countercation, the reductive carbonylation of $IrI_{3.4}$ has been also monitored by IR spectroscopy in a pressurized cylindrical internal reflectance (CIR) cell. Chlorobenzene/water mixtures (20:1) were employed for this purpose, at 130 °C and 5 bar of carbon monoxide for 2 h, leading to the formation of a mixture of species characterized by four bands at 2163 (w), 2112 (vs), 2064 (vs), and 1982 (m) $cm^{-1}$. Except for a shift due to the nature of the countercation, these bands could be attributed to $H[IrHI_3(CO)_2]$ at 2163 ($\nu_{Ir-H}$), 2112 and 2064 ($\nu_{CO}$); and to $H[IrI_2(CO)_2]$ at 2064 and 1982, with the 2064 $cm^{-1}$ band deriving from the contribution from (and superimposition of) the common band shown by both of the complexes. Therefore, we became interested in isolating this anionic $[IrHI_3(CO)_2]^-$ complex, which is reported as an intermediate species of the water-gas shift reaction in the literature, being slowly transformed into a mixture of $[IrI_4(CO)_2]^-$ and $[IrI_2(CO)_2]^-$ with $H_2$ evolution through a disproportionation process.[5] With rhodium, this side reaction takes a significant place and a mechanism has been proposed by Eisenberg and co-workers[25] from kinetic studies and quenching experiments. More recently, $[RhHI_3(CO)_2]^-$ was isolated and characterized.[26]

**[PPN][IrHI$_3$(CO)$_2$] (2).** A rapid and quantitative synthesis of this compound was accomplished via the slow addition of 1 equiv of aqueous HI to a $CH_2Cl_2$ solution of [PPN]-$[IrI_2(CO)_2]$. The reaction proceeds very cleanly (see Scheme 2). However, it is worth mentioning that Forster reported on the formation of significant amounts of $[IrI_4(CO)_2]^-$ when a slight excess of HI was added to the anionic iridium precursor in nitromethane.[5] We can confirm this piece of observation, i.e. that in $CH_2Cl_2$, after formation of equimolecular amounts of complex **2**, addition of even a slight excess of HI results in the generation of $[IrI_4(CO)_2]^-$, thus leading, with 1 mol in excess, to the complete transformation of the hydride species at the end of the reaction. Complex **2** has been crystallized as large dark orange crystals, and its X-ray crystal structure determined. The unit cell contains four $PPN^+$ cations and four $[IrHI_3(CO)_2]^-$ anions, the structure of which is discussed (Figure 2).

The two iodine atoms trans to the CO ligands, which can be considered as belonging to the equatorial plane, present two iridium−iodine distances of 2.6964(6) Å for Ir(I)−I(I) and 2.6927(5) Å for Ir(1)−I(2), i.e. about 0.05 Å longer than the mean Ir−I bond length in complex **1**. The axial Ir(1)−I(3) bond shows some lengthening due to the large trans-influence of the hydride ligand (Ir(1)−I(3) = 2.8360(6) Å). The three I−Ir−I angles, which are 91.563(18),

(25) Baker, E. C.; Hendriksen, D. N.; Eisenberg, R. *J. Am. Chem. Soc.* **1980**, *102*, 1020.
(26) Roe, D. C.; Sheridan, R. E.; Bunel, E. E. *J. Am. Chem. Soc.* **1994**, *116*, 1163.

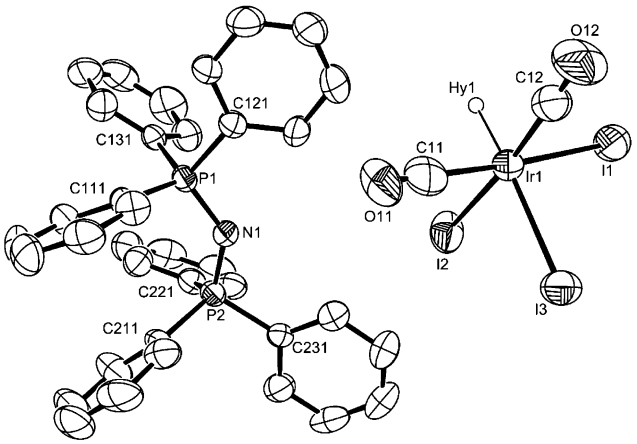


**Figure 2.** ORTEP drawing of [PPN][IrHI$_3$(CO)$_2$] (**2**). Ellipsoids are at the 50% probability level. The hydride ligand Hy1 has been positioned in its ideal position at 1.6 Å from Ir1.

**Scheme 2.** Schematic Diagram Showing the Whole Reactivity of the Anion [IrI$_2$(CO)$_2$]$^-$ toward HI and CH$_3$I and Then the Formation of the Neutral Dimer by Iodide Abstraction

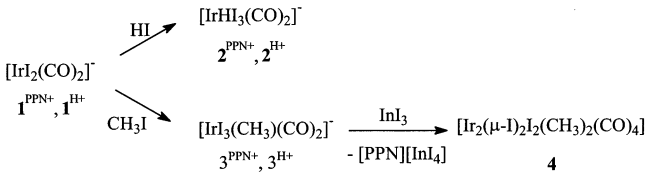


95.749(18), and 92.049(19)°, respectively, slightly deviate from 90° and are not very far to constitute a right-angled trihedron. Besides these three heavy atoms, the three remaining ligands are less precisely positioned in the relevant octahedron. As for the two CO's, the two iridium−oxygen distances are close one to the other, i.e., 2.955 Å for Ir(1)−O(11) and 2.985 Å for Ir(1)−O(12); the two carbon−iridium and two carbon−oxygen bond distances, as already observed in [IrI$_2$(CO)$_2$]$^-$, show the following values: Ir(1)−C(12) = 1.852(18) Å, C(12)−O(12) = 1.127(8) Å; Ir(1)−C(11) = 1.913(10) Å, C(11)−O(11) = 1.042(9) Å. The hydride ligand has been positioned in its ideal position, the sixth of the octahedron, and lies at a distance of about 1.6 Å from the iridium atom. Due to the uncertainty in the position of this hydrogen atom in the final refinements, it could be safer not to comment further on the Ir−H bond length, although it would have been interesting to compare this distance in an anionic mononuclear moiety to other ones that mainly belong to cationic structures. Indeed, in the three Ir(III) cationic complexes [IrH(OH)(PMe$_3$)$_4$]$^+$, [IrH(OMe)(PMe$_3$)$_4$]$^+$, and [IrH(SH)(PMe$_3$)$_4$]$^+$, the Ir−H distances are 1.71(8), 1.81(8), and 1.64(5) Å, respectively.[27] These bond distances lie in the range 1.5−2.0 Å reported for a mean iridium−hydride bond length.

In $^1$H NMR the hydride resonates at −11.63 ppm (−40 °C) in CD$_2$Cl$_2$. $^{13}$C-enriched **2** gives a signal at 155.0 ppm, but no coupling between the hydrogen nucleus and the two CO ligands has been observed.

As for IR spectra, the two CO stretching bands appear at 2103(s) and 2052(s) cm$^{-1}$, i.e. quite at higher frequencies than the two CO bands of the precursor **1** (2046 and 1967 cm$^{-1}$), the difference of 51 cm$^{-1}$ being consistent with the two CO ligands being in a mutual cis position.

(27) Milstein, D.; Calabrese, J. C.; Williams, I. D. *J. Am. Chem. Soc.* **1986**, *108*, 6387.

**Table 3.** Selected Infrared and NMR Data for Complexes **1**−**4**

| complex | $\nu_{CO}$, cm$^{-1}$ [a] | $\nu_{CO}$, cm$^{-1}$ [b] | $\delta_{^{13}CO}$, ppm[a] | $\delta_{^1H}$, ppm[a] |
|---|---|---|---|---|
| **1** | 2046 s, 1967 s | 2045 s, 2034 s, 1968 s, 1960 s | 169.9 | |
| **2** | 2157 w, 2103 s, 2052 s | | 155.0 | −11.65 |
| **3** | 2100 s, 2048 s | 2088 s, 2034 s | 156.0, 15.75 (*CH$_3$*) | 2.15 |
| **4** | 2120 s, 2074 s | | 152.5, 150.4, 150.1 | 1.96, 1.90 |

[a] In CH$_2$Cl$_2$. [b] In KI.

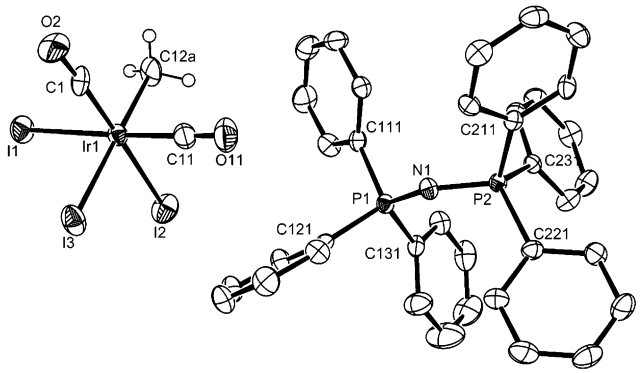


**Figure 3.** ORTEP plot of the mononuclear structure of [PPN][IrI$_3$(CH$_3$)(CO)$_2$] (**3**) (major form), with the labeling scheme for the anion. Ellipsoids are at the 50% probability level.

The corresponding rhodium hydride complex [RhHI$_3$(CO)$_2$]$^-$ was previously reported[26] to be stable only below −20 °C and to undergo disproportionation at room temperature to provide [RhI$_4$(CO)$_2$]$^-$, [RhI$_2$(CO)$_2$]$^-$, and dihydrogen. The same disproportionation path has been proposed by Forster[5] for the iridium analogue. Relevant NMR data for the rhodium complex that are worthy of note are −10.45 ppm for the hydride and 177.9 ppm for the $^{13}$CO ligands; infrared data do only show a CO band at 2080 cm$^{-1}$, and the Rh−H band has not been detected. All the shifts of the hydride and the CO's observed in NMR spectra point to a more nucleophilic character of the iridium metal center than that of the rhodium one.

All of the NMR data obtained (Table 3) are in agreement with those recently reported by Merbach et al.[10] for this complex in solution, pointing to a *fac,cis* geometry. FAB-MS spectra in negative mode show the molecular peak at *m*/*z* 631 and two main signals corresponding to the successive loss of two CO ligands.

**[PPN][IrI$_3$(CH$_3$)(CO)$_2$] (3).** In accordance with earlier reports,[12a] complex **1** reacts quickly with an excess (40 equiv) of iodomethane to provide [IrI$_3$(CH$_3$)(CO)$_2$]$^-$ quantitatively. This orange compound crystallizes in the space group $P2_1/c$ ($Z$ = 4), the asymmetric unit containing one PPN cation, the anion [IrI$_3$(CH$_3$)(CO)$_2$]$^-$, and a CH$_2$Cl$_2$ solvent molecule. In the anion there is a disorder between one CO and the methyl ligands which corresponds to the ratio 0.67:0.33. The [IrI$_3$(CH$_3$)(CO)$_2$]$^-$ moiety shows a fac arrangement with a pseudooctahedral geometry. The two iridium−iodine

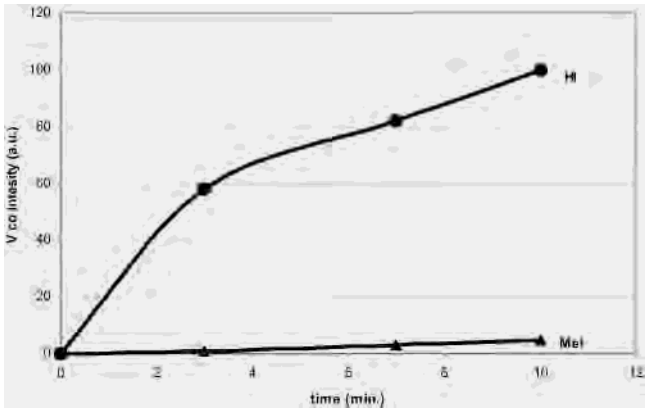


**Figure 4.** Kinetic measurements of the formation of **2** or **3** resulting from the oxidative addition of HI or $CH_3I$ to $[IrI_2(CO)_2]^-$ (anion of **1**).

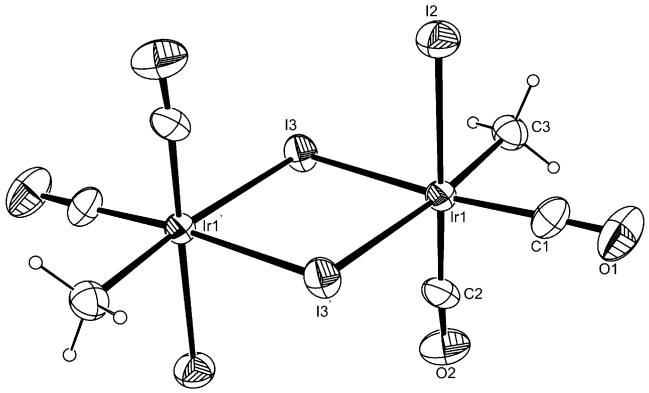


**Figure 5.** ORTEP drawing of $[Ir(\mu\text{-}I)_2I_2(CH_3)_2(CO)_4]$ (**4**) with the labeling scheme, the primed atoms being deduced from the first half-molecule through the inversion center. Ellipsoids are at the 50% probability level.

bond distances trans to the two CO ligands, which measure 2.7005(4) and 2.7177(4) Å, respectively, are slightly increased (~0.05−0.06 Å) with respect to the mean value of 2.65 Å observed in $[IrI_2(CO)_2]^-$ . Far more significant is the lengthening of the Ir(1)−I(2) bond trans to the methyl ligand since its distance, which can be accounted for by the trans-influence of the methyl group, is 2.7658(4) Å. The infrared spectra of $[PPN][IrI_3(CH_3)(CO)_2]$ (**3**) present two stretching bands at 2100(s) and 2048(s) $cm^{-1}$ in $CH_2Cl_2$ solutions, the difference of 52 $cm^{-1}$ between the two wavenumbers being consistent with two CO ligands in mutual cis-position.

In $^1H$ NMR **3** is characterized by a singlet at 2.15 ppm ($CD_2Cl_2$), and the $^{13}C$ NMR spectra for $[IrI_3(CH_3)(^{13}CO)_2]^-$ and $[IrI_3(^{13}CH_3)(CO)_2]^-$ present a singlet at −15.75 ppm for the methyl group and a singlet at 156.0 ppm for the carbonyl group. These values fit those previously reported.[21]

**Competitive Oxidative Addition Reactions of HI and $CH_3I$ on $[PPN][IrI_2(CO)_2]$.** As previously proposed by Forster,[5] although the complex $[IrI_3(CH_3)(CO)_2]^-$ is usually considered as the resting state in the iridium-catalyzed carbonylation of methanol, the competitive oxidative addition of HI is a very fast process that gives a relatively unstable species, whereas the reaction of $CH_3I$ onto $[IrI_2(CO)_2]^-$ occurs at a relatively slower rate to produce the stable **3** complex.

Even on addition of 40 equiv of $CH_3I$, the reaction rate of the oxidative addition to **1** is slower than that observed when using the stoichiometric quantity of HI required to react with the anion $[IrI_2(CO)_2]^-$. Experimental evidence concerning a reaction mixture of $HI/CH_3I/[IrI_2(CO)_2]^-$ (1:40:1) clearly indicates that HI reacts faster than $CH_3I$, the kinetic curve being superimposed on that of HI alone, the hydride **2** being the only one detected (Figure 4).

To shed light on these markedly different reaction rates, we carried out competitive experiments using a reaction mixture of $HI/CH_3I/[PPN][IrI_2(CO)_2]$ (1:40:1). Infrared monitoring of this experiment followed by comparison with the two independent oxidative additions gave confirmation that complex **1** reacts quickly and exclusively with HI to provide **2**. Even with solutions standing overnight at room temperature, $CH_3I$ does not add to form complex **3**, and $[PPN][IrI_4(CO)_2]$ and **2** are the only observed species. However, on heating at 160 °C the same reaction mixture, addition of $CH_3I$ slowly occurs to form **3** at the expense of **2**. Thus, the regeneration of **1** from **2** described by Forster[5] might occur only at relatively high temperatures. It constitutes a very important step within the mechanism of methanol carbonylation, which intervenes prior to the commonly accepted oxidative addition of $CH_3I$. Moreover, the presence of water under a CO atmosphere is also a way to restore $[IrI_2(CO)_2]^-$ from $[IrHI_3(CO)_2]^-$ via the water-gas shift reaction.[5]

**$[Ir_2(\mu\text{-}I)_2I_2(CH_3)_2(CO)_4]$ (4).** Concerning the iridium mechanism of the catalytic methanol carbonylation, two cycles are interconnected which involve anionic and neutral intermediate species, respectively. Maitlis et al. have shown that the cis-migratory insertion of carbon monoxide into the iridium−methyl bond occurs faster in the neutral intermediate.[28,29] Under the operative conditions of the Cativa process, one of the main roles of the ruthenium halo carbonyl complex is to promote the formation of the neutral species $[IrI_2(CH_3)(CO)_3]$, via iodide abstraction.[30] Thus, by adding $InI_3$ (1 equiv/Ir) as iodide scavenger, we prepared $[Ir_2(\mu\text{-}I)_2I_2(CH_3)_2(CO)_4]$ (**4**) with moderate yields. Extraction with hot cyclohexane, followed by recrystallization, gave orange crystals of **4**, albeit in poor yields, suitable for X-ray analysis. This complex crystallizes in the $P\bar{1}$ space group with half of the dinuclear moiety in the asymmetric unit (Figure 5).

The dimer is centrosymmetric, with two iodide and two CO ligands in the axial positions and two methyl and two CO groups in the equatorial terminal ones. The two octahedrons are completed and bridged by two iodide ligands. Bond lengths are consistent with those observed for complex **3**, except for the distances Ir−I of the bridging iodides, for which a slight lengthening is observed. In particular, the Ir(1)−I(3) trans to CO and Ir(1)−I(3′) trans to $CH_3$ bond distances are 2.7156 (11) and 2.8021 (11) Å, respectively.

It should be mentioned that Haynes et al., in a preliminary communication, reported the synthesis of **4** performed by

(28) Pearson, J. M.; Haynes, A.; Morris, G. E.; Sunley, G. J.; Maitlis, P. M. *J. Chem. Soc., Chem. Commun.* **1995**, 1045.
(29) Haynes, A.; Pearson, J. M.; Vickers, P. W.; Charmant, J. P. H.; Maitlis, P. M. *Inorg. Chim. Acta* **1998**, 382.
(30) Whyman, R.; Wright, A. P.; Iggo, J. A.; Heaton, B. T. *J. Chem. Soc., Dalton Trans.* **2002**, 771.

reacting $InI_3$ with $[NBu_4][IrI_3(CH_3)(CO)_2]$ and described its reactivity with carbon monoxide to provide $[IrI_2(CH_3)(CO)_3]$;[22] in a note, they indicated that an X-ray structure of **4** was in progress and that the iridium−(bridging) iodide distances were 2.799 (2) and 2.716 (2) Å with a methyl and a CO ligand in trans-position, respectively.

Infrared spectra in $CH_2Cl_2$ solutions show two CO bands at 2120 (vs) and 2074 (vs) $cm^{-1}$ corresponding to the 2 $A_u$ IR-active modes for the dinuclear complex. Thus, the positions of these two stretching frequencies relevant to the centrosymmetric dimer cannot be compared with the two corresponding CO bands for **3** (A′ and A″ modes), which are observed at 2100 and 2048 $cm^{-1}$. In $^1H$ NMR spectra the methyl groups give a singlet mainly at 1.96 ppm and one peak of lower intensity at 1.90 ppm, which could be assigned to a different isomer of the centrosymmetric complex **4**. In $^{13}C$ NMR spectra for $^{13}CO$-enriched **4**, a strong signal is obtained at 152.5 ppm together with a less intense one at 150.4 and a third peak of weak intensity at 150.1 ppm. No coupling has been detected between the two differently positioned cis $^{13}CO$ ligands. Due to their quite different intensities, these three signals might be assigned to two isomers of the main complex, the structure of which has been determined.

## Conclusion

The oxidative addition of HI to the square-planar complex $[PPN][IrI_2(CO)_2]$ is a very fast reaction that affords the hydrido iodo carbonyl derivative $[PPN][IrHI_3(CO)_2]$. The corresponding methyl complex $[PPN][IrI_3(CH_3)(CO)_2]$ has been prepared by addition of MeI to the Ir(I) precursor. Removal of one iodide ligand from the latter complex does afford the neutral dimeric species $[Ir_2(\mu\text{-}I)_2I_2(CH_3)_2(CO)_4]$. All the aforementioned four compounds have been fully characterized by X-ray diffractometry besides IR and $^1H$ and $^{13}C$ NMR spectroscopies.

**Supporting Information Available:** X-ray crystallographic data in CIF format. This material is available free of charge via the Internet at http://pubs.acs.org.

IC0340938